H/D exchange in *N*-heterocycles catalysed by an NHC-supported ruthenium complex

V. H. Mai,[a] O. B. Gadzhiev,[b] S. K. Ignatov,[b] and G. I. Nikonov[a]

[a] Chemistry Department, Brock University, 1812 Sir Isaac Brock Way, St. Catharines, ON L2S 3A1, Canada

[b] Chemistry Department, N. I. Lobachevsky State University of Nizhny Novgorod, Gagarin Avenue 23, 603950, Nizhny Novgorod, Russia

Corresponding Author
* Georgii Nikonov, gnikonov@brocku.ca

Supporting Information

1 General Information

All manipulations were performed using conventional glove box or nitrogen-line Schlenk techniques. Solvents were pre-dried by using Grubbs-type purification columns and stored in ampoules equipped with a Teflon valve. Deuterated solvents were dried over sodium, potassium or CaH_2 as appropriate, distilled under reduced pressure and stored in ampoules with a Teflon valve. NMR samples were prepared in New Era tubes equipped with J. Young-type Teflon valves. NMR spectra were obtained with Bruker DPX-400 and Brucker DPX-600 instruments ([1]H: 400 and 600 MHz; [13]C: 100.6 and 151 MHz) spectrometers at 298 K. ^{1}H and ^{13}C NMR spectra were referenced internally to residual protiosolvent (^{1}H) or solvent (^{13}C) resonances and are reported relative to tetramethylsilane (δ=0 ppm). Chemical shifts are quoted in δ[ppm] and coupling constants in Hertz. IR spectra were recorded by using a PerkinElmer 1600 FTIR spectrometer as Nujol mulls between NaCl windows. All chemicals were purchased from Sigma– Aldrich and Alfa Aesar were used without further purification. C_6D_6 was purchased from Cambridge Isotope Laboratories and were dried over K/Na alloy before use. Complexes $Cp(IPr)RuH_3$ (**1**), $Cp(PPh_3)RuH_3$ (**2**), $Cp(PiPr_3)RuH_3$ (**3**), $Cp(IPr)RuH_2(SiH_2Ph)$ (**4**), $Cp(IPr)RuH_2(SiHMePh)$ (**5**) $Cp(IPr)RuH_2(SiMeCl_2)$ (**6**) were synthesized by literature procedures.[1-3]

2 Experimental Details

2.1 Catalyst synthesis, general scheme.

For Cp based catalysts L = IPr, IMes, PiPr$_3$, PPh$_3$
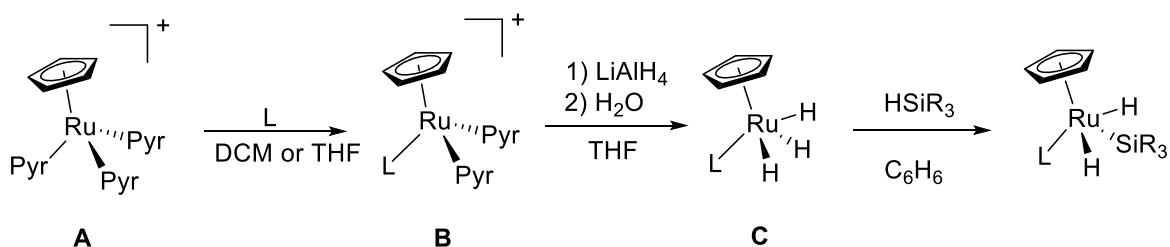
For Cp* based catalysts L = IPr, IMes
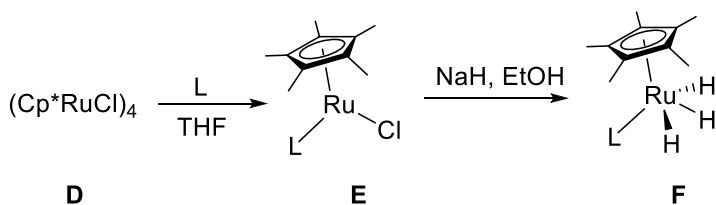
Scheme S1. Preparation of polyhydride half-sandwich ruthenium complexes.

$Cp*(IPr)RuH_3$ (**7**), $Cp(IMes)RuH_3$ (**8**), $Cp*(IMes)RuH_3$ (**9**) were prepared by applying procedures developed for **1**-**3**.[1,2,3]

2.1.1 General procedure for Cp systems (**1, 2, 3, 8**):

1) To a solution of [CpRu(pyr)$_3$][PF$_6$] (A) (0.5 mmol) in 20 mL of dichloromethane was added NHC carbene (0.5 mmol) (NHC= IPr, IMes, IiPr). After stirring at room temperature for 8h, the resulting solution was dried to yield [Cp(NHC)Ru(pyr)$_2$][PF$_6$] (**B**) as a brownish-yellow, air sensitive solid. This compound was used for the next steps without any further purification.

2) To a solution of [Cp(NHC)Ru(pyr)$_2$][PF$_6$] (**B**, 0.36 mmol) in 20 mL of isopropanol was added 1.2 equivalent of KOtBu (0.43 mmol). After stirring at room temperature for 3 h, the resulting solution was dried, extracted by hexane, and then re-crystalized from a mixture of toluene/hexane (1:3) to give the target Cp(NHC)RuH$_3$ (**C**).

2.1.2 General procedure for Cp* systems (**7, 9**):

1) To a solution of [Cp*RuCl]$_4$ (**D**) (0.5 mmol) in 20 mL THF was added 0.5 mmol of NHC (NHC = IPr, IMes). After stirring at room temperature for 24 h, the resulting purple solution was dried to yield the corresponding unsaturated 16e Cp*(NHC)RuCl (**E**) as a brownish-yellow, air sensitive solid. This new compound was used in the next step without any further purification.

2) To a solution of Cp*(NHC)RuCl (**E**) (0.4 mmol) in 20 mL of ethanol was added 1.2 equivalent of NaH (0.48 mmol). After stirring at room temperature for 12 h, the resulting solution was dried, the residue was extracted by hexane, and then re-crystalized from a mixture of toluene/hexane (1:3) to give the corresponding Cp*(NHC)RuH$_3$ (**F**).

2.2 Catalyst characterization:

Cp*(IPr)RuH$_3$ (**7**)

To a solution of 0.26 g (0.40 mmol) of Cp*(IPr)RuCl in 20 mL in ethanol was added 1.2 equivalent of NaH (0.012g, 0.48 mmol). After stirring at room temperature for 12h, the resulting solution was dried, extracted by hexane, and then re-crystalized at room temperature from 8 mL mixture of toluene/hexane (3:1) by slow evaporation to yield 0.15 g (60%) of Cp*(IPr)RuH$_3$. IR (Nujol): ν(Ru–H) = 2030 cm^{-1}. ^{1}H NMR (600 MHz, C$_6$D$_6$): δ -9.53 (s, 3H, RuH_3), 1.07 (d J(H-H)=6.7 Hz, 12 H, CH_3 of ^{i}Pr), 1.52 (d, J(H-H)=6.7 Hz, 12 H, CH_3 of ^{i}Pr), 1.8 (s, 15 H, CH_3 of Cp*) 2.93 (sep, J(H-H)=6.7Hz, 4H, CH of ^{i}Pr), 6.44 (s, 2 H, NCH), 7.21-7.31 (m, 6H, C$_6H_3$). ^{13}C NMR (151 MHz, C$_6$D$_6$): 12.6 (s, CH$_3$ of Cp*), δ 28.5 (s, CH$_3$), 28.8 (s, CH(CH$_3$)$_2$), 93.4 (s, C ring of Cp*), 122.6 (s, NCH), 124.2 (m-C, C$_6$H$_3$), 129.2 (p-C, C_6H$_3$), 140.3 (s, o-C$_6$H$_3$), 146.7 (s, N-C$_6$H$_3$), 197.13 (Ru-CN$_2$).

S4

Anal. Cal. for $C_{37}H_{55}RuN_2$ (628.92): C, 70.66; H, 8.81; N: 4.45. Found: C, 70.27, H, 8.71; N, 4.06.

Cp(IMes)RuH₃ (8)

To 0.230 g (0.30 mmol) of [Cp(IMes)Ru(pyr)₂][PF₆] in 20 mL in isopropanol solution was added 0.040 g (0.36 mmol) of KO^{t}Bu. After stirring at room temperature for 3h, the solution was dried, extracted by hexane, and then re-crystalized at room temperature from a 5mL mixture of toluene/hexane (2 : 3 v/v) by slow evaporation to give Cp(IMes)RuH₃ as a hexane solvate. Yield: 0.146 g (87%). IR (Nujol): ν(Ru–H) = 2016 cm^{-1}. ^{1}H NMR (600 MHz, C_6D_6): δ -9.92 (s, 3H, RuH), 2.12 (s, 12H, 2 ortho CH_3 of mesityl), 2.13 (s, 6H, 1 para CH_3 of mesityl), 4.57 (s, 5H, Cp), 6.12 (s, 2H, NCH), 6.8 (s, 4H, C_6H_2). ^{13}C NMR (151 MHz, C_6D_6): δ 18.44 (s, oCH_3 of mesityl), 20.89 (pCH_3 of mesityl), 81.0 (C ring of Cp), 120.2 (NCH), 129.2 (s, m-C_6H_2), 136.25 (s, p-C_6H_2), 137.9 (s, o-C_6H_2), 139.2 (s, N-C_6H_2); 193.4 (Ru-CN₂).

Anal. Cal. for Cp(IMes)RuH₃*hexane, $C_{32}H_{46}RuN_2$ (559.8): C, 68.66; H, 8.28; N, 5.00. Found: C, 68.60, H, 8.55; N, 4.99.

Cp*(IMes)RuH₃ (9)

Preparation and characterization of **9** have been reported: A. L. Jones, G. S. McGrady, P. Sirsch, J. W. Steed, *Chem. Commun.* **2005**, 5994.

IR (Nujol): ν(Ru–H) =2023 cm^{-1}. ^{1}H NMR (600 MHz, C_6D_6): δ -9.39 (s, 3H, RuH), 1.84 (s, 15H, CH_3 of Cp*), 2.13 (s, 12H, 2 ortho CH_3 of mesityl), 2.19 (s, 6H, 1 para CH_3 of mesityl), 6.12 (s, 2H, NCH), 6.88 (s, 4H, C_6H_2). ^{13}C NMR (151 MHz, C_6D_6): δ 12.5 (s, CH_3 of Cp*), 18.9 (s, oCH_3 of mesityl), 20.9 (pCH_3 of mesityl), 78.9 (C ring of Cp*), 120.5 (NCH), 129.2 (s, m-C_6H_2), 135.9 (s, p-C_6H_2), 194.3 (Ru-CN₂).

Cp(IMes)₂RuH (10)

To a solution of Cp(IMes)RuH₃ (0.018 g, 0.04 mmol) in 5 mL in benzene was added 3 equivalents of IMes (0.034 mg, 0.12 mmol). After stirring at 50ºC for 24h, the resulting solution was dried. The residue was extracted by ether, filtered through a Celite column, and then re-crystalized from a mixture of diethyl ether and hexane (4:1, v/v) to give the corresponding Cp(IMes)₂RuH.

IR (Nujol): ν(Ru–H) = 2012 cm^{-1}. ^{1}H NMR (600 MHz, C_6D_6) δ -11.93 (s,1H, RuH), 2.11 (s, 12H, 1 ortho CH_3 of mesityl), 2.15 (s, 12H, 1 ortho CH_3 of mesityl), 2.25 (s, 12H, 1 para CH_3 of mesityl), 4.29 (s, 5H, Cp), 6.21(s, 4H, NCH), 6.76 (s, 4H, mC_6H_2), 6.86 (s, 4H, mC_6H_2). ^{13}C NMR (151 MHz, C_6D_6): δ 14.1 (s, o-CH_3 of mesityl), 18.9 and 18,3 (s, o-CH_3 of mesityl), 20.9 and 22,8 (pCH_3 of mesityl), 31,8 (pCH_3 of mesityl), 82.4 (C ring of Cp), 123,1 (NCH), 129.3 (NCH), 129.4 (NCH), 136.7 (s, m-C_6H_2), 137.2 (s, m-C_6H_2), 138.4 (s, p-C_6H_2), 139.2 (s, p-C_6H_2), 159,5 (s, N-C_6H_2); 186,2.6 (Ru-CN₂). 203.6 (Ru-CN₂).

2.3 Catalytic H/D exchange reaction:

Stock solutions of **1, 2, 3, 7, 8, 9** and **10** were prepared in C_6D_6 before use. Substrates was added to NMR tubes in a glove box. The degree of deuteration was monitored by ^{1}H-NMR.

3 Selected NMR Spectra

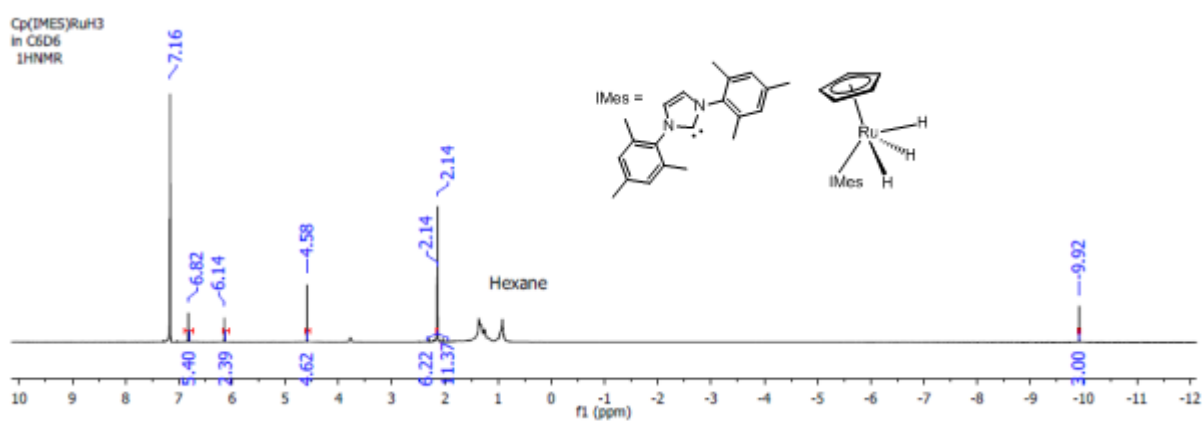## 3.1 NMR spectra of new tris(hydride) ruthenium complexes
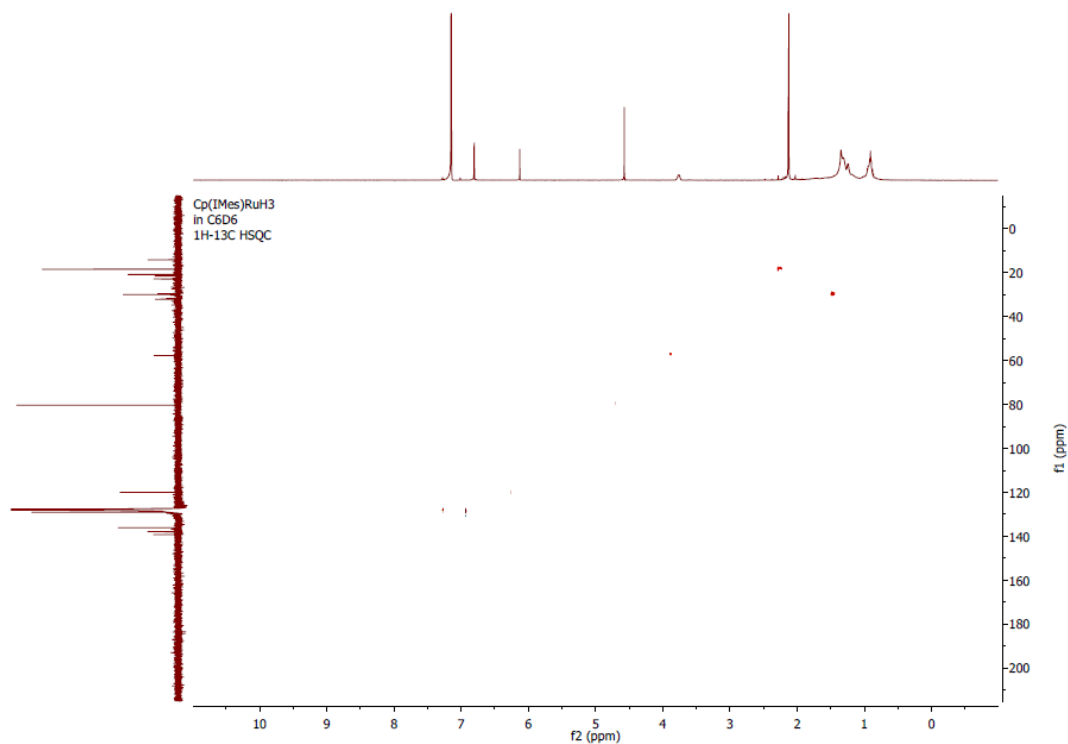
Cp(IMes)RuH₃

Figure S1. ^{1}H NMR (600 MHz, C_6D_6) of **Cp(IMes)RuH₃**.

Figure S2. ^{1}H- ^{13}C HSQC NMR (600 MHz, C_6D_6) of **Cp(IMes)RuH₃**.

Cp(IMES)RuH3
in C6D6
13C{1H}NMR
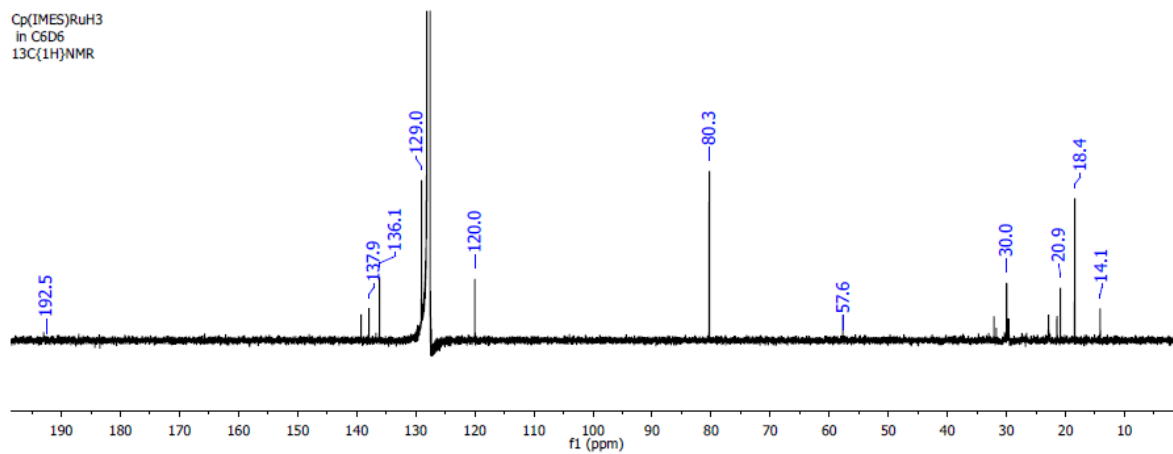
Figure S3. $^{13}\text{C}\{^1\text{H}\}$ NMR spectrum (151 MHz, C_6D_6) of **Cp(IMes)RuH₃**.

1H NMR spectra of Cp*(IPr)RuH3 in C6D6
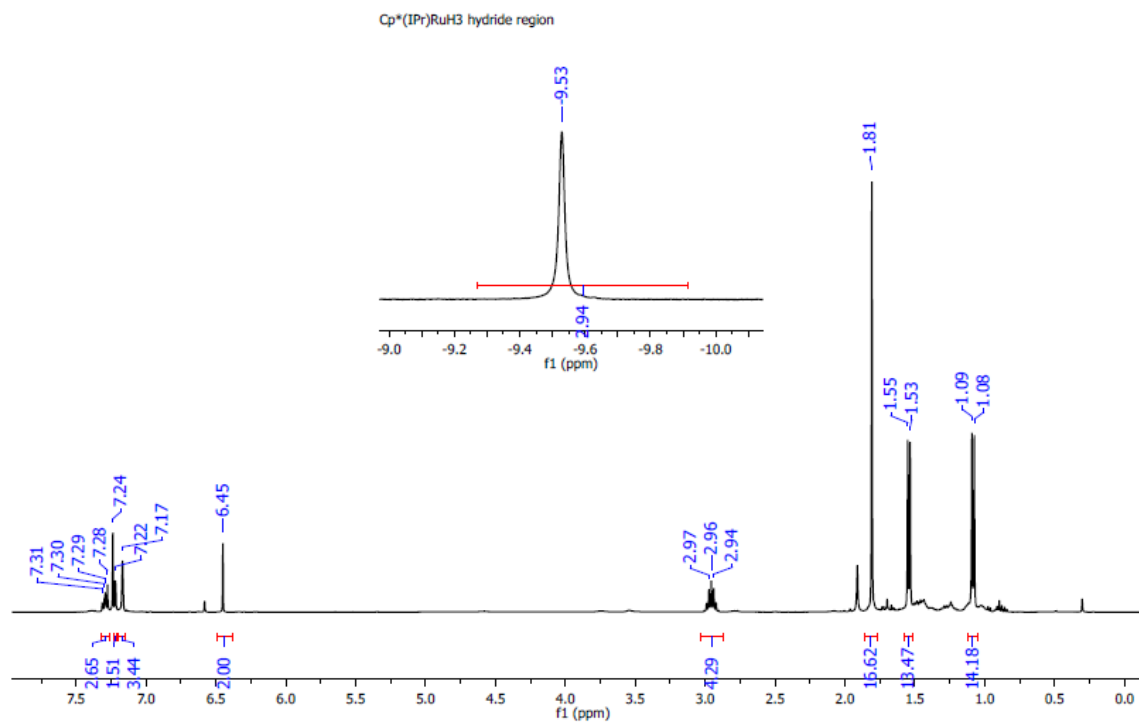
Figure S4. ^{1}H NMR (600 MHz, C$_6$D$_6$) of **Cp*(IPr)RuH₃**.
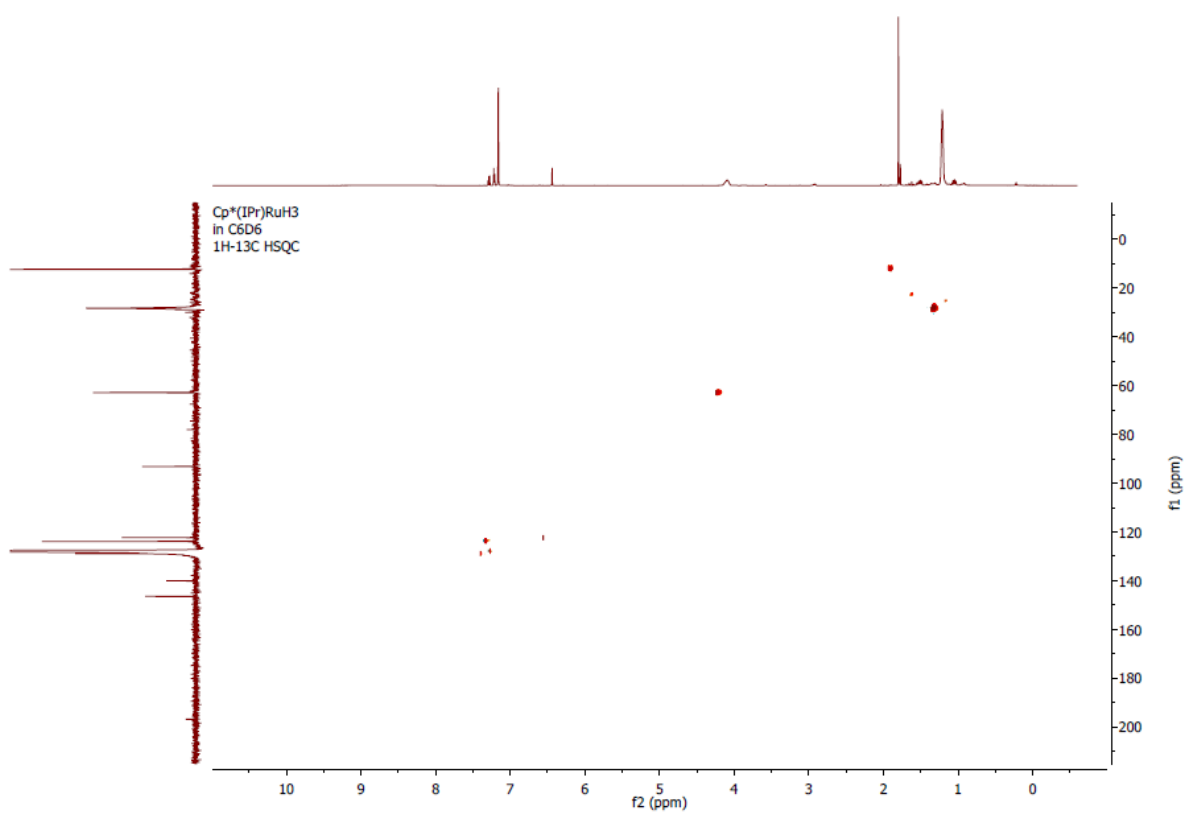
Figure S5. ^{1}H- ^{13}C HSQC NMR (600 MHz, C$_6$D$_6$) of Cp*(IPr)RuH$_3$.   S

Cp*(IPr)RuH3
in C6D6
13C{1H}NMR
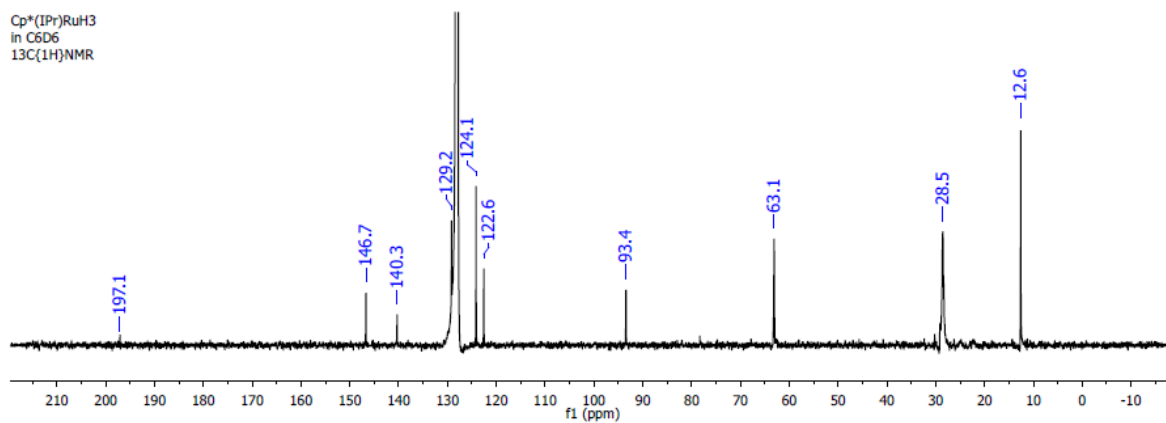
Figure S6. $^{13}C\{^1H\}$ NMR spectrum (151 MHz, C_6D_6) of **Cp*(IPr)RuH₃**.

Cp(IMes)₂RuH
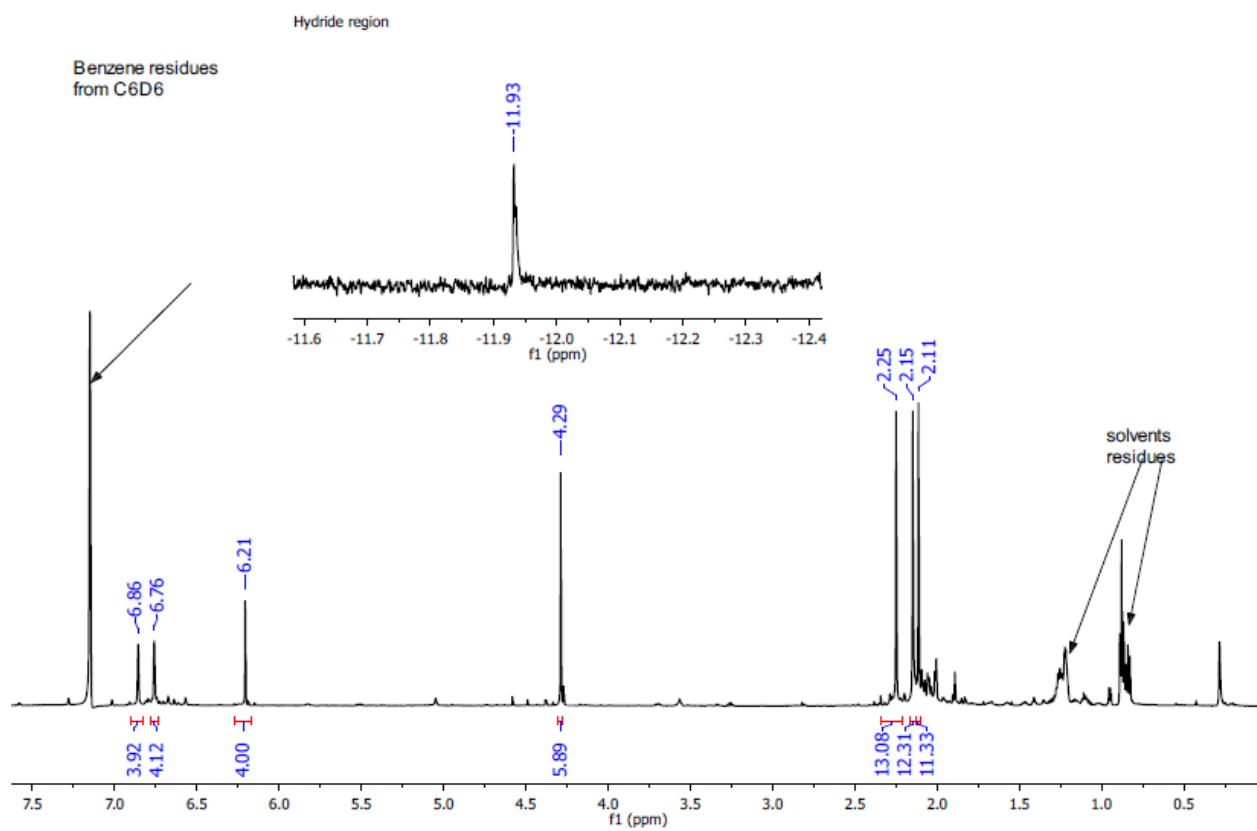
Figure S8. ^{1}H NMR (600 MHz, C₆D₆) of **Cp(IMes)₂RuH**.
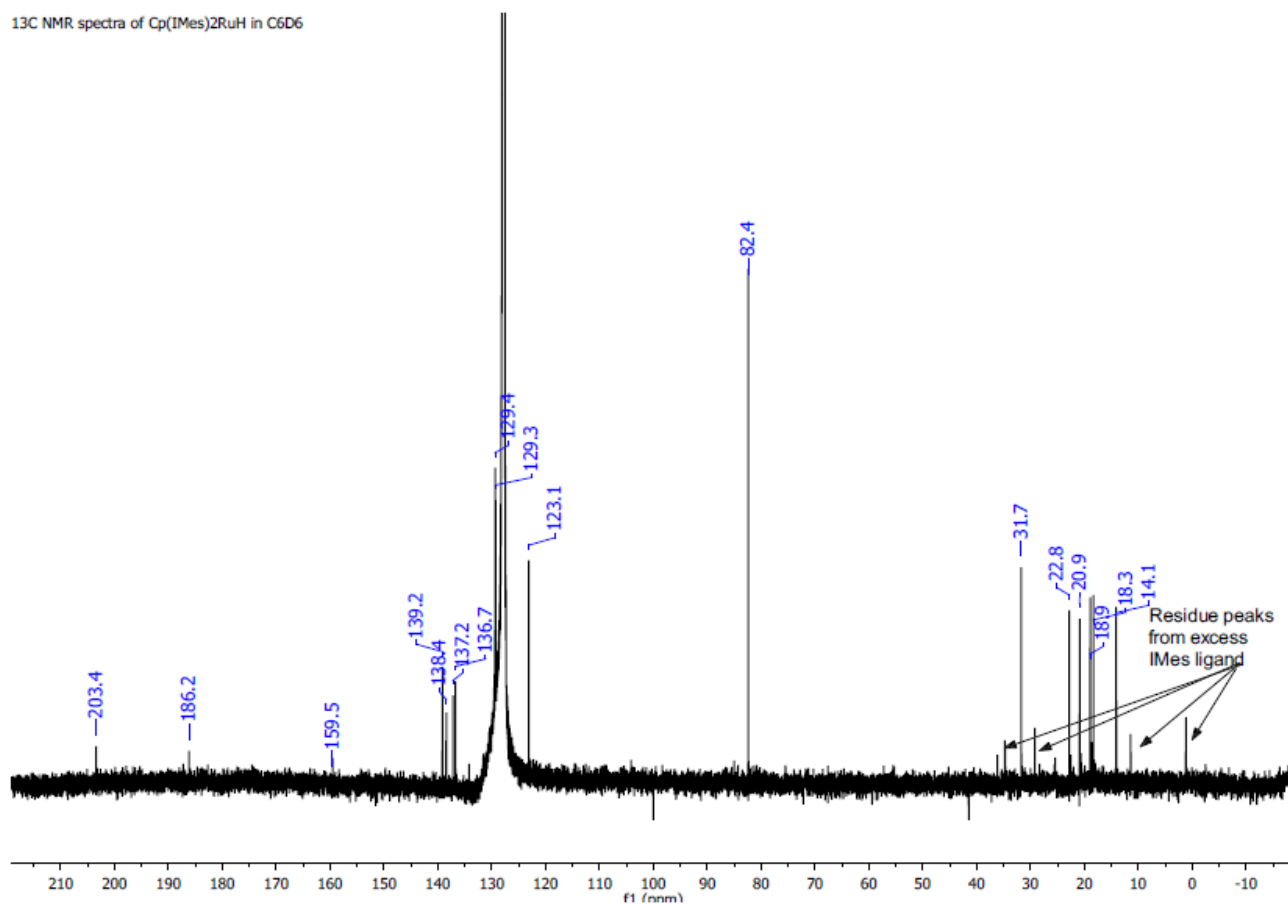
Figure S9. $^{13}C\{^1H\}$ NMR spectrum (151 MHz, C_6D_6) of **Cp(IMes)₂RuH**.

Figure S10. The overlap of ^1H NMR spectra of **Cp(IMes)RuH₃** (red) and **Cp(IMes)₂RuH** (green).

3.2 Selected stacked NMR spectra to analyse the degree of deuteration in H/D exchange reactions.

3.2.1 Spectra showing the progress of H/D exchange:

Toluene
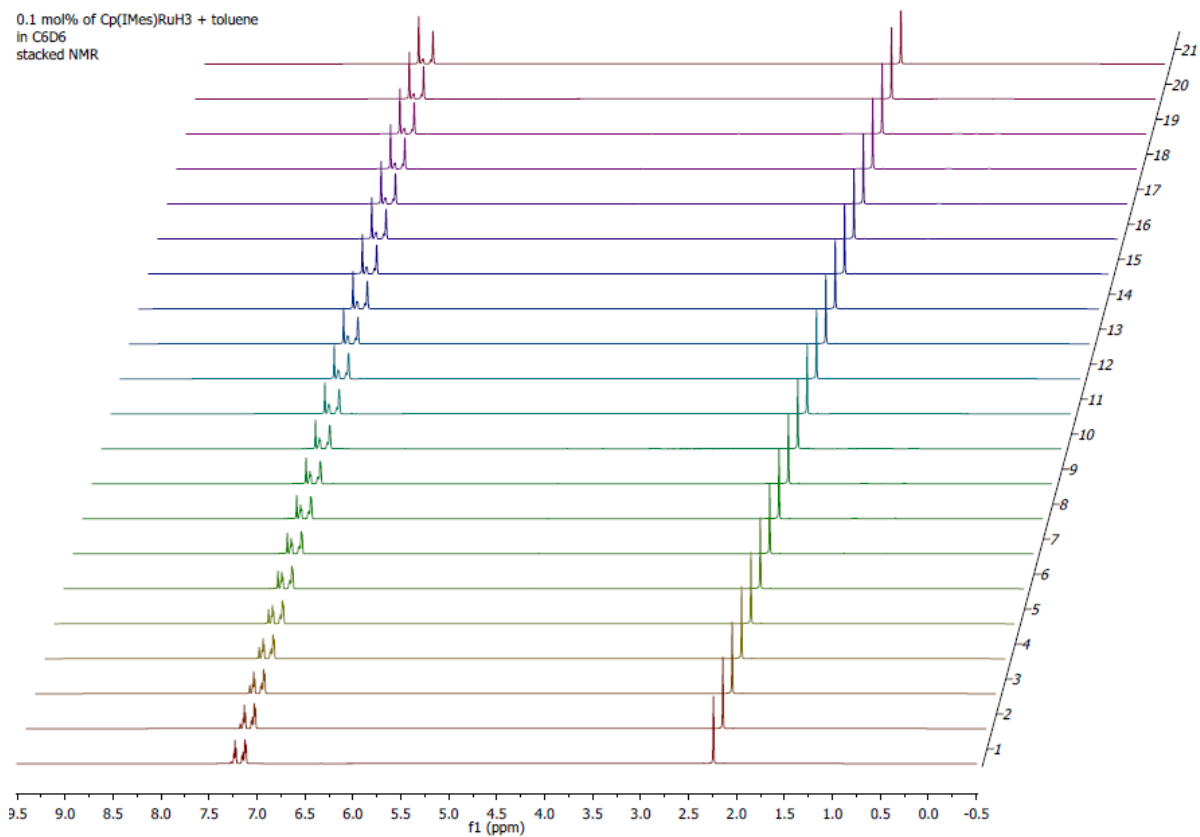
Quinoline

0.1 mol% of Cp(IMes)RuH3
in C6D6 + quinoline in C6D6
stacked NMR
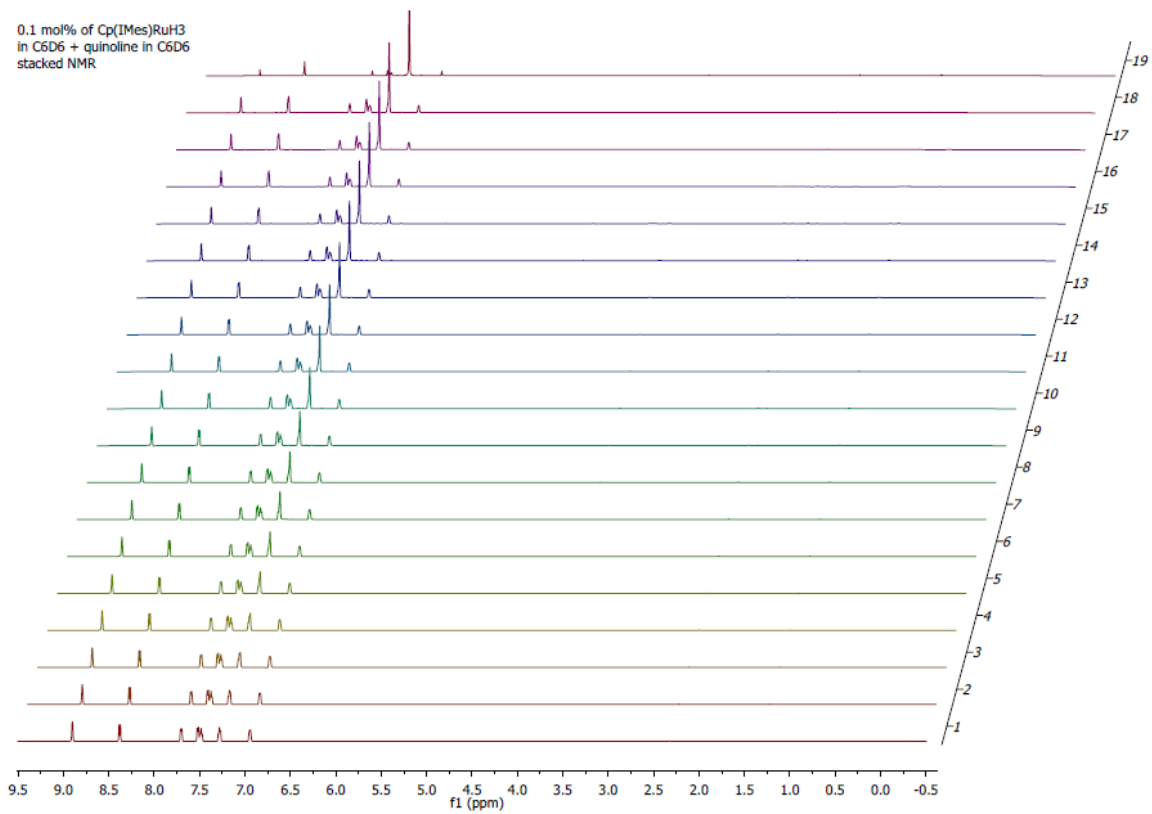
Naphthalene

0.1 mol% of Cp(IMes)RuH3 + naphthalene
in C6D6
stacked NMR

Acridine

S15

Phenanthridine

0.1 mol% of Cp(IMes)RuH3 + phenanthridine
in C6D6
stacked NMR
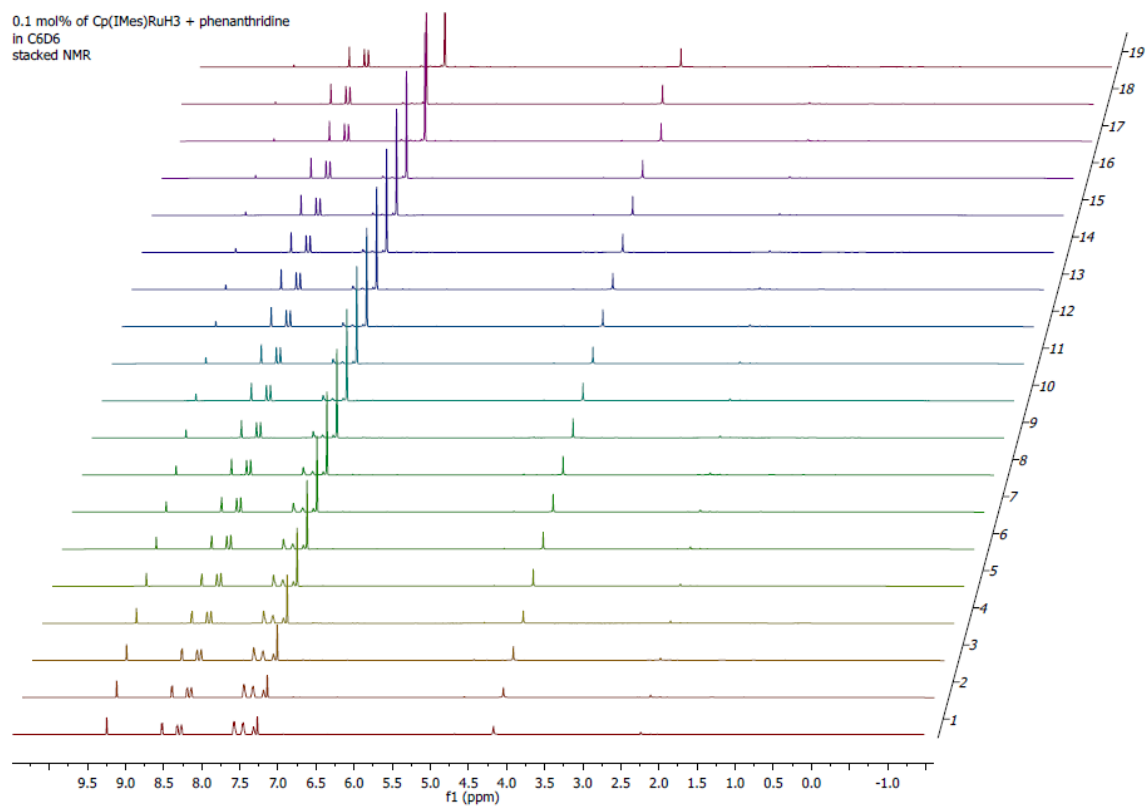
2,6 lutidine

0.1 mol% of Cp(IMes)RuH3 + 2,6 lutidine
in C6D6
stacked NMR
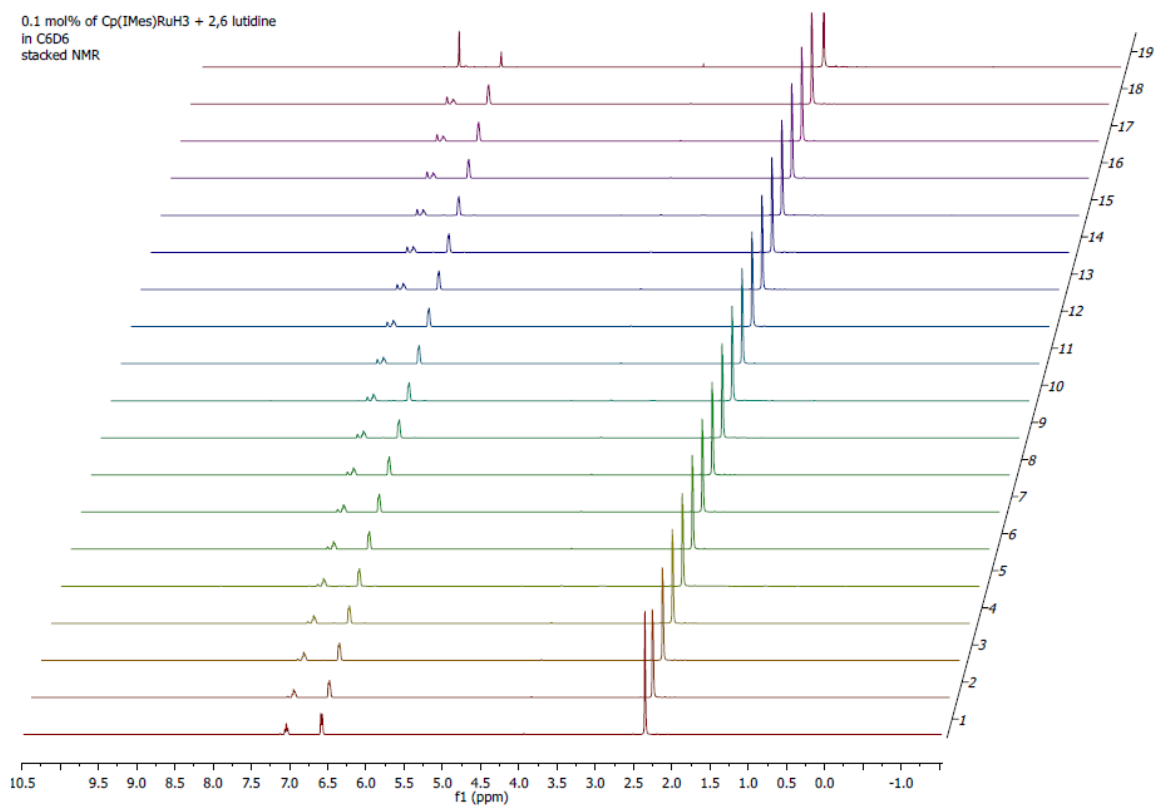
Phenyl quinoline

0.1 mol% of Cp(IMes)RuH3 + phenylquinoline
in C6D6
stacked NMR
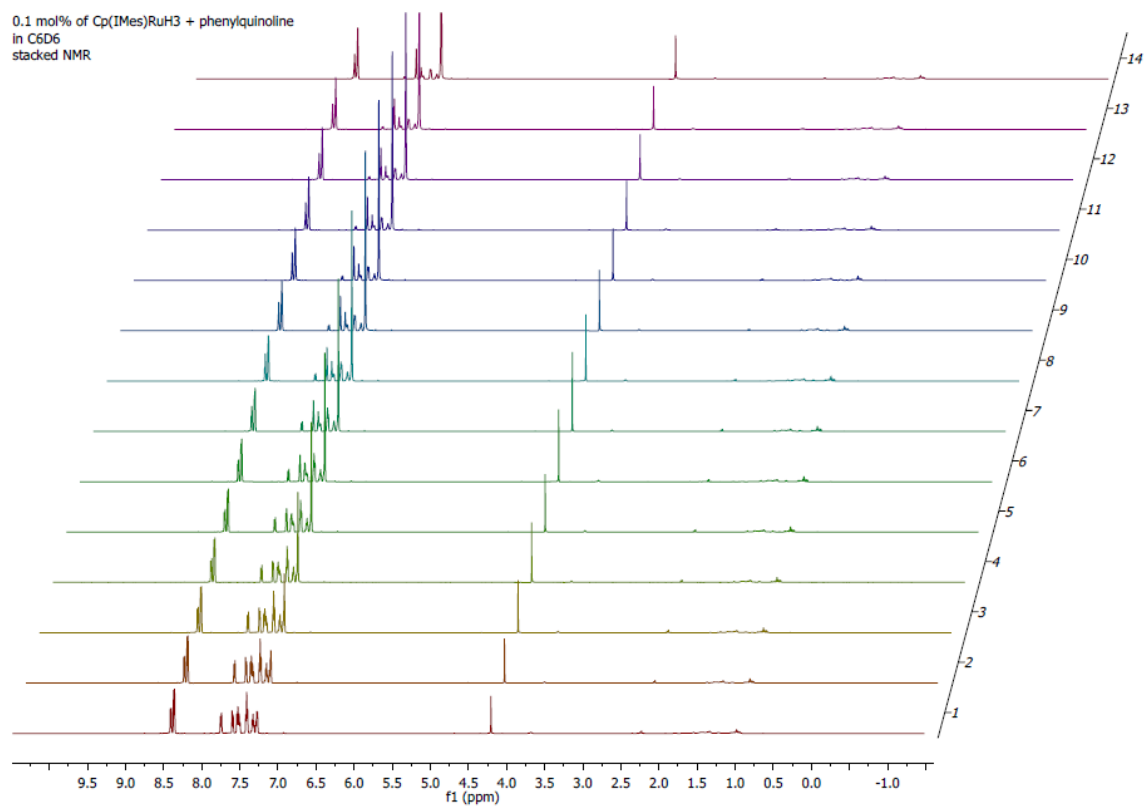
Pyrazine

0.1 mol % of Cp(IMes)H3 + pyrazine
in C6D6
stacked NMR
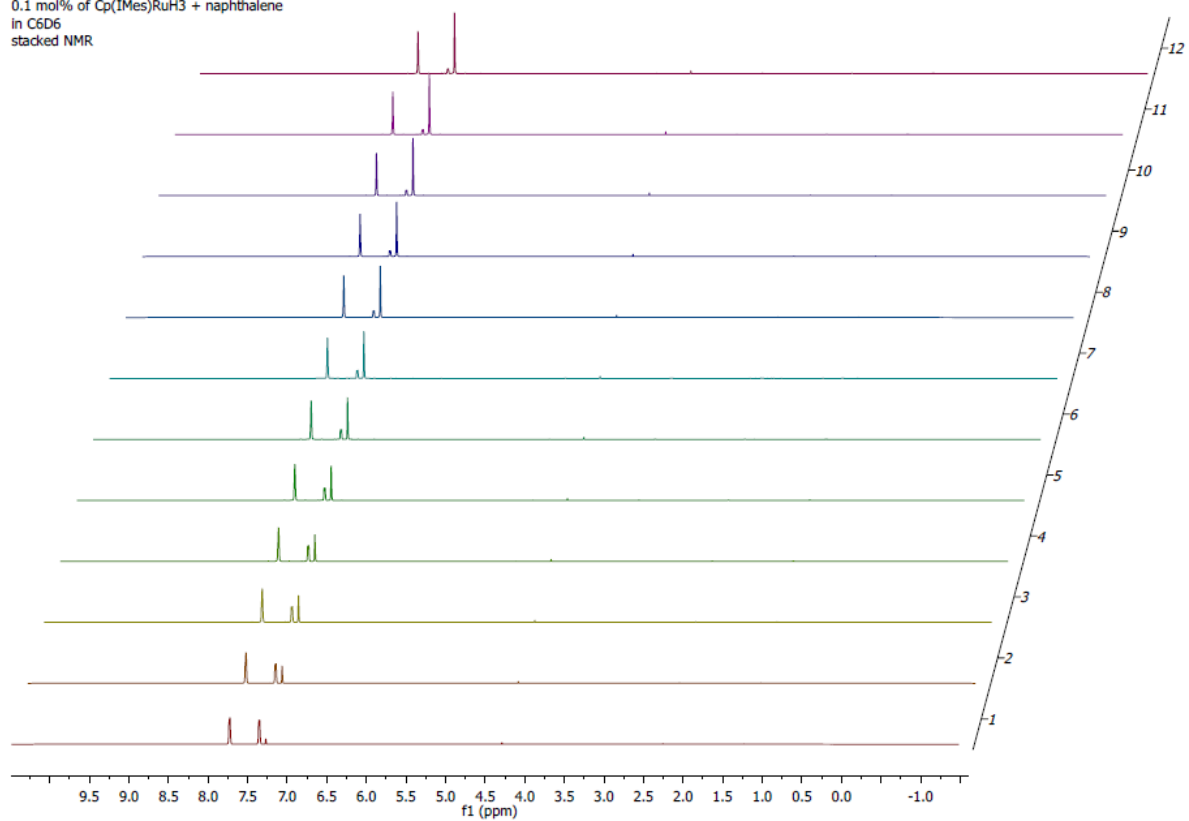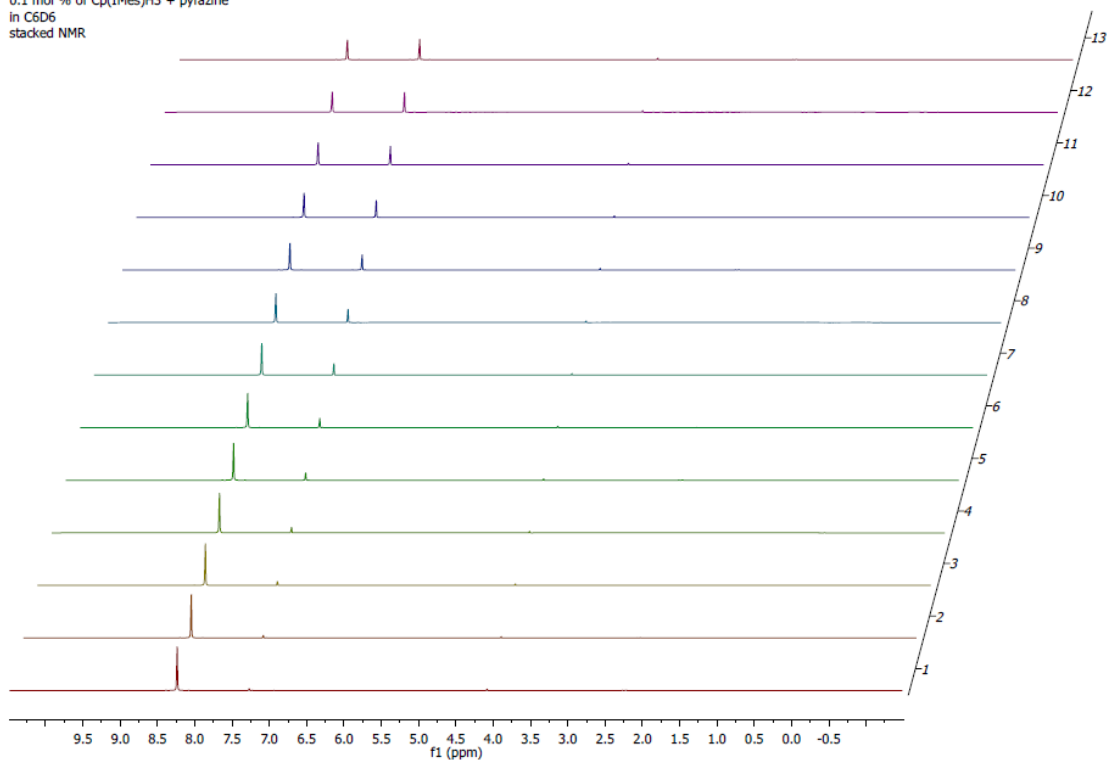

the NMR
progress of the
catalytic H/D
exchange
reaction using
Cp(IMes)2RuH
as catalyst (0.1
mol%) and
pyridine as
substrate in
C6D6 with
ferrocene insert

pyridine
peaks
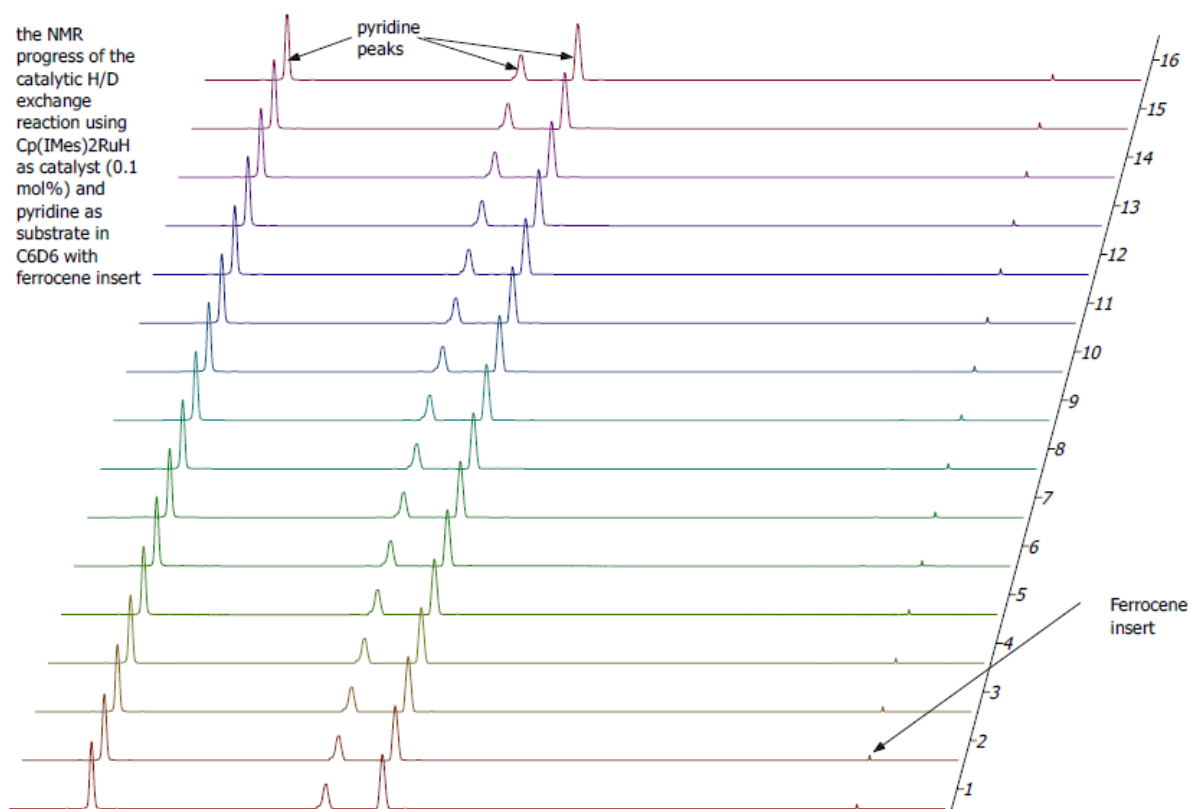
Ferrocene
insert

Figure S11. The NMR progress of catalytic H/D exchange reaction using Cp(IMes)$_2$RuH as catalyst and pyridine as substrate in C$_6$D$_6$ with ferrocene insert.

Figure S12. The catalytic reaction with 0.1 mol % of Cp(IMes)₂RuH in C₆D₆, with added pyridine, with ferrocene insert.

4 DFT calculation

All calculations were performed with Gaussian 03.[11]

C-H activation in methane, ethane, benzene, and pyridine was studied.

1) For methane, two paths, with the lateral and central attacks, were revealed (Table S1 and Figure S13). It is interesting, that the topology of the PES for the C-H activation step in the both the lateral and central attacks is quite complex and involves bifurcation points and the corresponding reaction paths branching as well as non-branching paths.
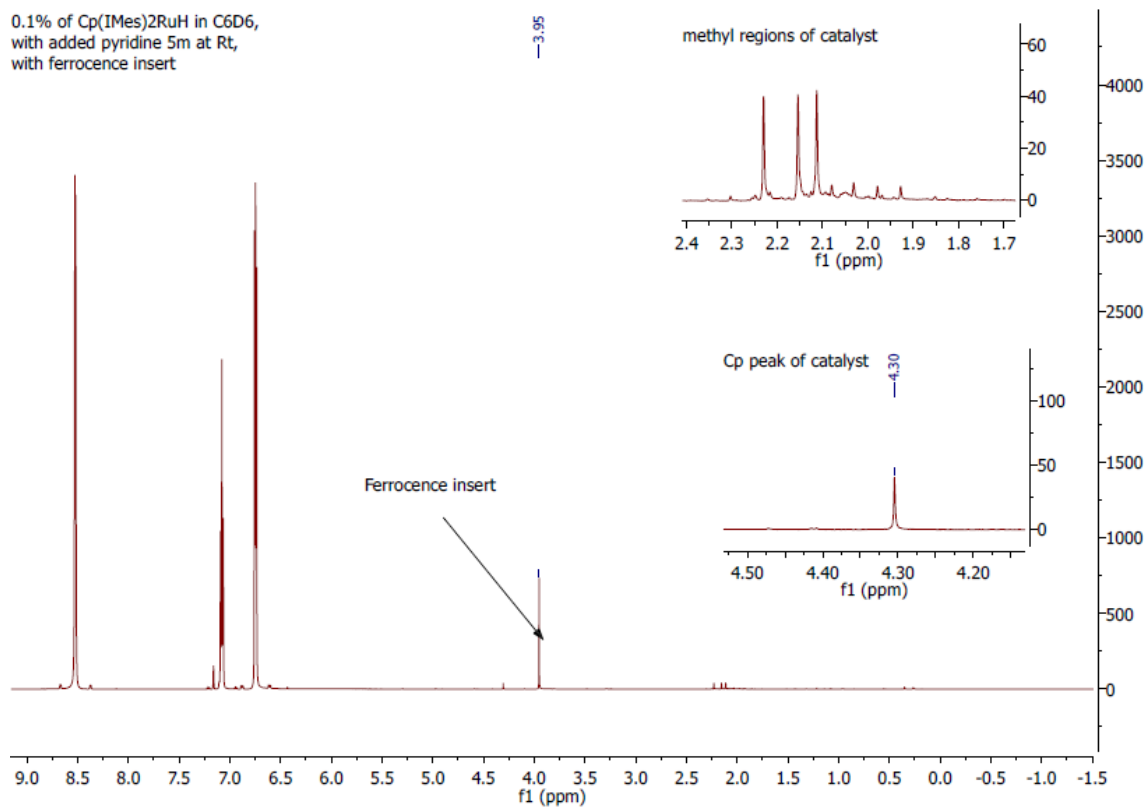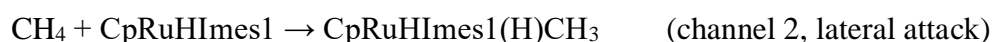
$$CH_4 + CpRuHImes1 \rightarrow CpRuHImes1CH_3H \qquad \text{(channel 1, central attack)}$$
$$CH_4 + CpRuHImes1 \rightarrow CpRuHImes1(H)CH_3 \qquad \text{(channel 2, lateral attack)}$$

Indeed, in the case of methane activation without bifurcation, the IRC curve connects the transition state directly with the reactants' valley. In the opposite case, from the TS for C-H bond cleavage (Figure S13) the IRC calculations converge to another stationary point (Figure S13) with the relative energies about of 4.5 kcal/mol relative to the isolated Cp(L)RuH and CH_4. In each case, the obtained in the IRC and verified next by conventional TS localization stationary point was assigned to be a saddle point characterized by a soft imaginary vibrational mode about of 21i cm^{-1} with synchronous Cp ring rotation and CH_4 and Ru-H motion (Figure 3b).

Table S1. Energies of transition states relative to isolated reactants (CpRuHImes1 and CH4)

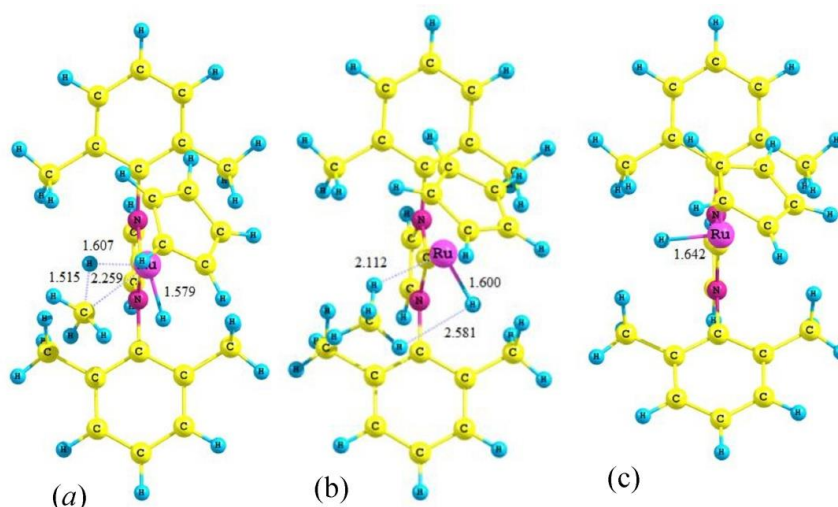| without branching		with branching, kcal/mol	
1a	2a	1b	2b
14.82	18.32	15.9	15.5
–	–	4.47	4.54

(a)   (b)   (c)

Figure S13. The transition state structure for the central attack with the branching in the reaction path (a), transition state in the branching in the reaction path (b), and the given comparison parental catalytic molecule (c). Bond lengths are given in Å.
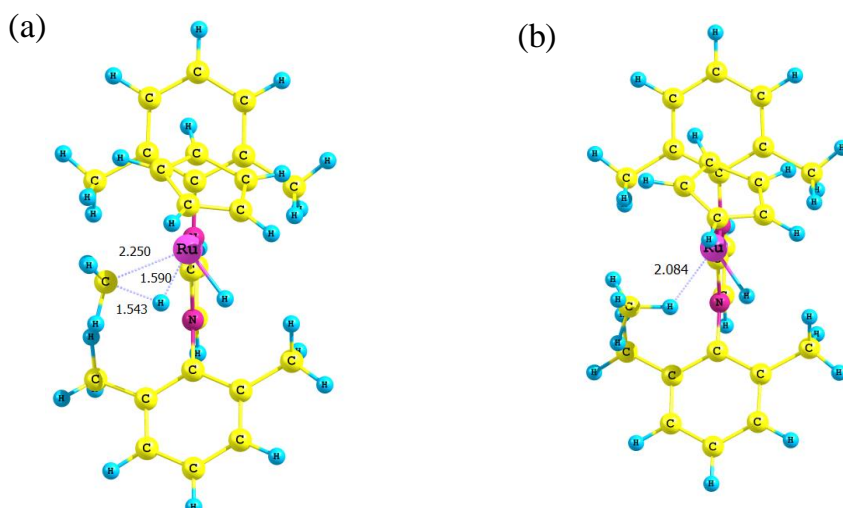

(a)

(b)

Figure S14. The transition state structure for the lateral attack with the branching in the reaction path (a) and transition state in the branching in the reaction path (b). Bond lengths are given in Å.

(a)

(b)
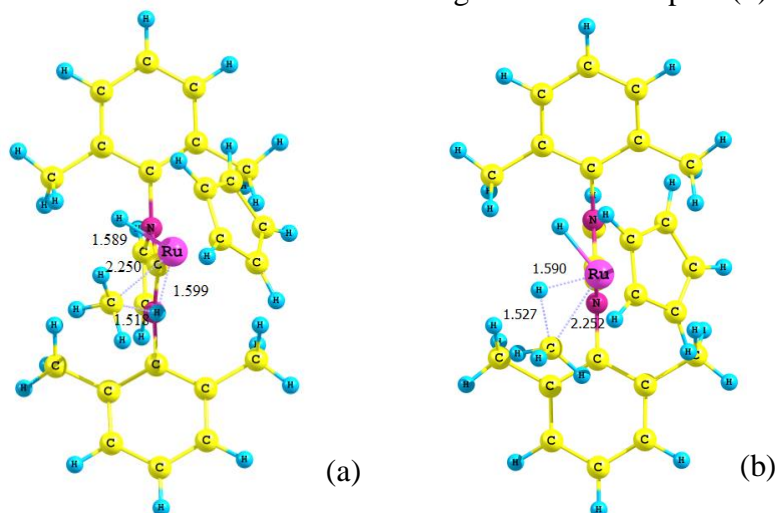
Figure S15. The transition state structure for the central (a) and lateral (b) attacks without branching in the reaction path. Bond lengths are given in Å.

For the paths 1a and 2a, i.e., without branching, the activation energies are 14.82 and 18.32 kcal/mol above isolated reactants, respectively. The activation energies of the corresponding channels 1b and 2b are 15.9 (15.8) and 15.5 (15.5) kcal/mol, respectively, where the data obtained at the B3LYP/A level are indicated in parentheses to be compared easily with those ones calculated at the

B3LYP/B theory level. Influence of expansion and augmentation of the basic sets for C/H/N was found to be negligible if the 6-311++G(d,p) and 6-31G(d,p) basis sets are considered.

The concept of the bifurcation points was introduced in [4-7]. More details related to the practical aspects were considered in [8-10].
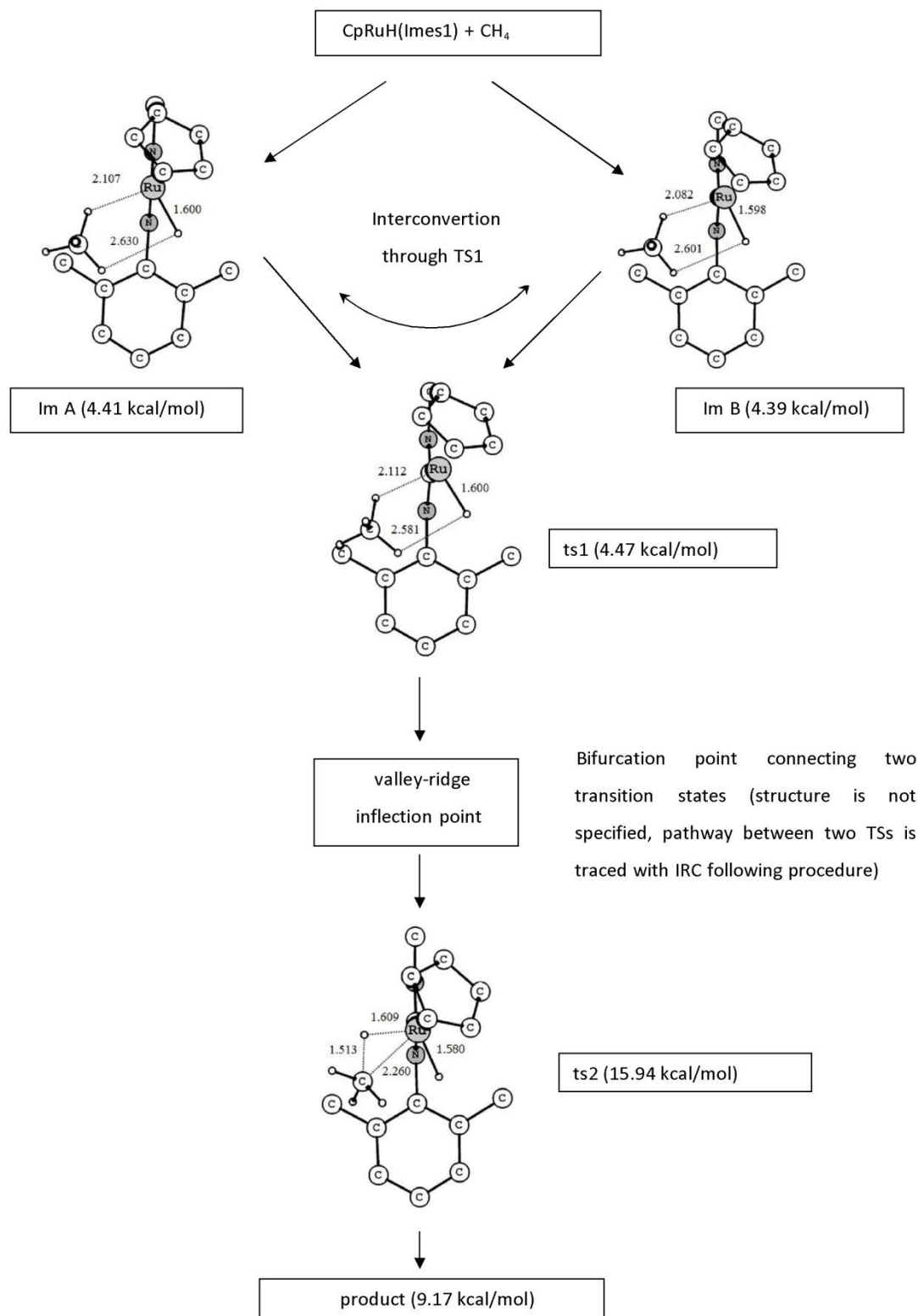

Figure S16. Central attack of CH_4 to Cp(L)(H)Ru occurring through the branching point.
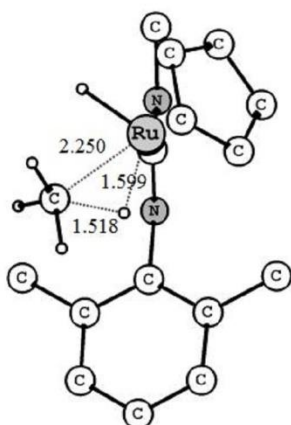
| CpRuH(Imes1) + CH$_4$ | → | ts1 (14.82 kcal/mol) | → | product(path no bif.) 8.33 kcal/mol |
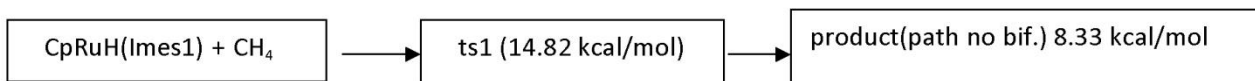
Figure S17. Central attack of CH$_4$ to Cp(L)(H)Ru occurring without reaction path branching.

2) For ethane also two paths, of lateral and central attacks, were revealed where addition occurs in a single step or two steps with an intermediate (Figure S18 and Table S2), as well as conformational isomers for different orientation of CH$_3$-group in the ethane.
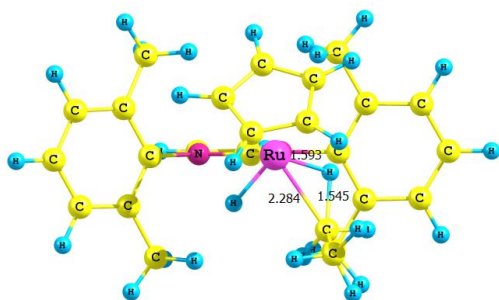
*path 1 –*1-TS1$_{C2H6}$
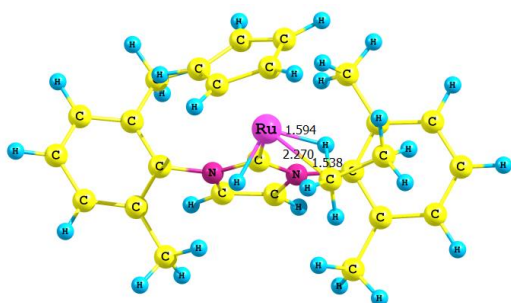
path 1 – 1-TS2$_{C2H6}$

path 1 – 1-TS3$_{C2H6}$

path 1 – 1-TS4$_{C2H6}$
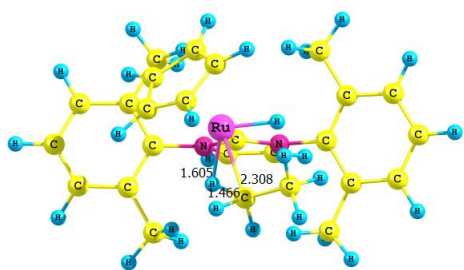
path 2 – 2-TS1$_{C2H6}$
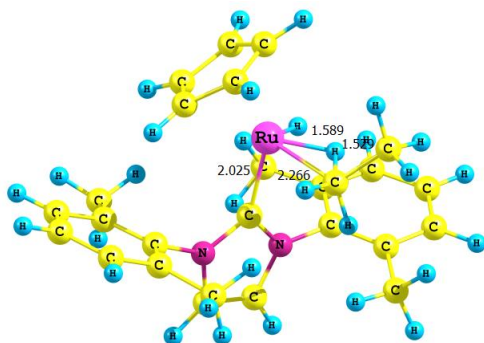
path 2 – 2-TS2$_{C2H6}$
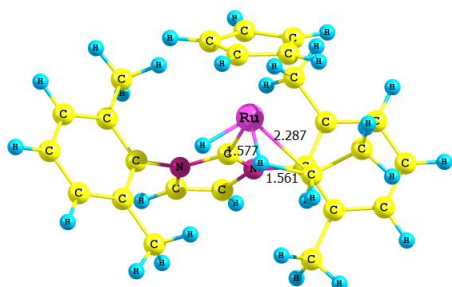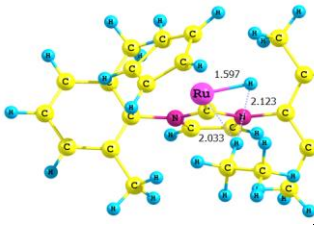
Figure S18. Transition states and ethane oxidative addition. Bond lengths are given in Å.

Table S2. Total (Etot) and relative (Erel(isolated reactants)) energies for transition states and complexes in the ethane addition reaction.
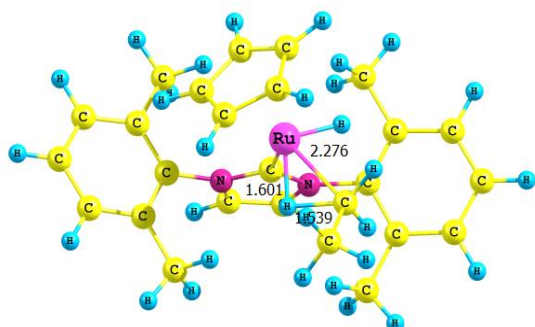
path 1 – central attack stationary point	Etot, a.u. (Erel(isolated reactants), kcal/mol)	*path 1 – central attack stationary point*	Etot, a.u. (Erel(isolated reactants), kcal/mol)
1-TS1$_{C2H6}$	-1213.406271 (17.78)	1-TS2$_{C2H6}$	-1213.408962 (16.09)
1-TS3$_{C2H6}$	-1213.407474	1-TS4$_{C2H6}$	-1213.403527

	(17.03)		(19.50)
complex, no bifurcation		complex, no bifurcation	
path 2 – lateral attack		*path 2 – lateral attack*	
2-TS1$_{C2H6}$	-1213.407569 (16.97)	2-TS2$_{C2H6}$	-1213.397542 (23.26)
complex, no bifurcation	-1213.427658 (4.36)		

3) For benzene, only the central attack was shown at the B3LYP/B theory level (Table S3 and Figure S17). The reaction is two-step, with two saddle points and one intermediate

$$C_6H_6 + CpRuH\text{-}Imes1 \rightarrow TS1_{C6H6} \rightarrow complex\ (im1_{C6H6}) \rightarrow TS2_{C6H6} \rightarrow product(im2_{C6H6})$$
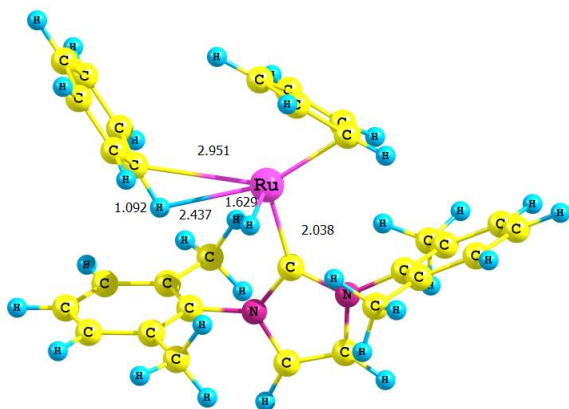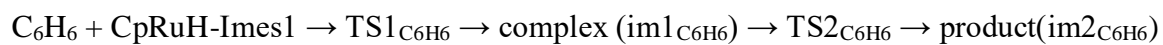
TS1$_{C6H6}$

im1$_{C6H6}$
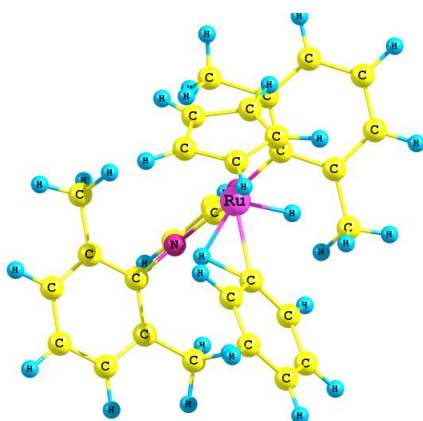
TS2$_{C6H6}$
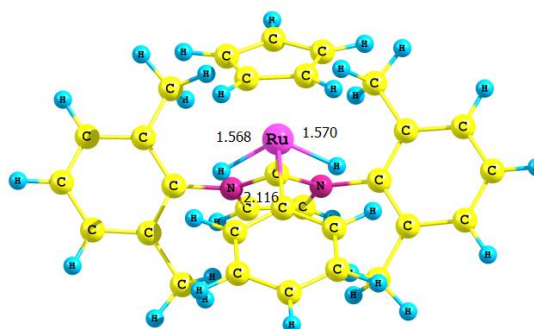
im2$_{C6H6}$

Figure S19 Transition states and intermediates for oxidative addition of benzene. Bond lengths are given in Å.

Table S3. Total (Etot) and relative (Erel(isolated reactants)) energies for transition states and complexes in the benzene addition reaction.
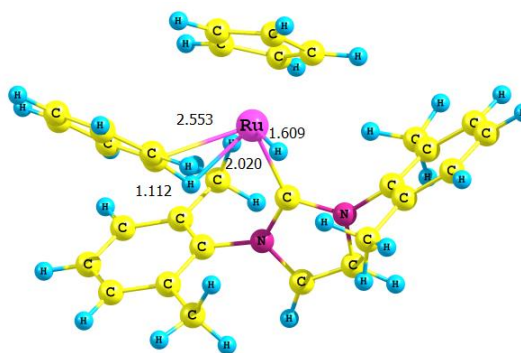
Stationary point	Etot, a.u. (Erel(isolated reactants), kcal/mol)
im2	-1365.844433 (6.05)
TS2	-1365.837315 (10.51)
im1	-1365.848369 (3.58)
TS1	-1365.846854 (4.53)

4) C-H activation in pyridine proceeds in two stages involving formation of intermediates shown in Chart S1. The energy profiles are shown in Figure S20.

$$CpRuHImes1 + C_6H_5N \rightarrow CpRuHImes1C_6H_5N$$

path 1-1   path 1-1a

path 2-1   path 2-1a

path 3
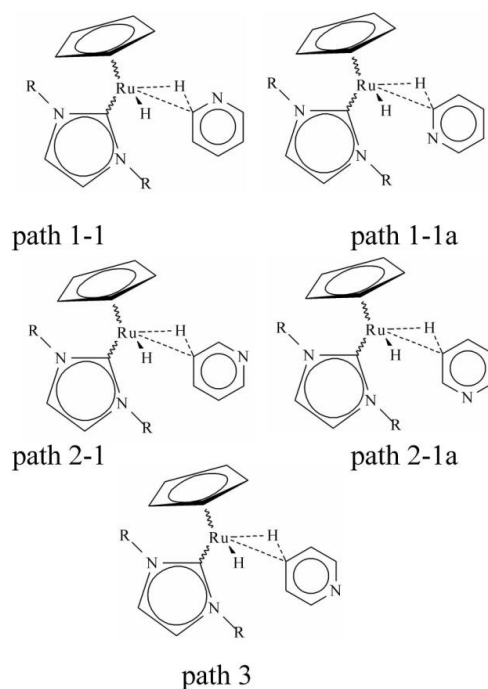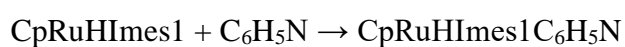
Chart S1. Transition states for various reaction channels of the oxidative addition pyridine to CpRuH(Imes1).

Table S4. Stepwise reaction paths and corresponding activation energies calculated at the B3LYP/B theory level. Step 1 is activated generation of corresponding pre-reactive complex, step 2 is a catalytic oxidative addition.

Reaction pathways	Activation energy, kcal/mol	
	step 1	step 2
path 1-1	5.26 (+1.54)	1.35
path 1-1a	3.72	4.08 (+2.73)
path 2-1	3.91 (+0.19)	5.60 (+4.25)
path 2-1a	4.24 (+0.52)	5.02 (+3.67)
path 3	4.33 (+0.61)	4.00 (+2.65)
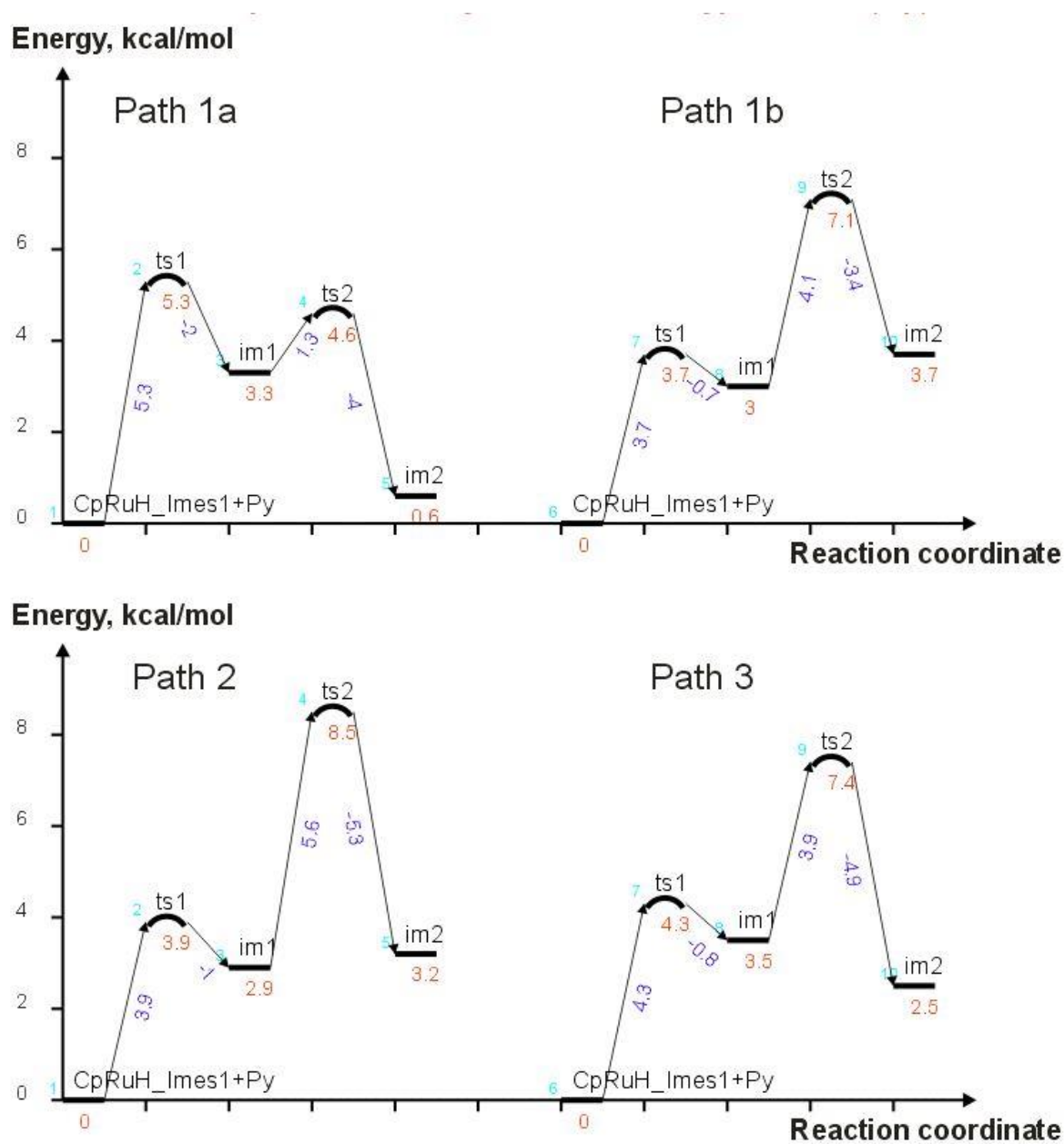
Figure S20. Relative energy profile for pyridine addition reaction catalyzed by Cp(L)RuH for the channels 1a, 1b, 2, and 3.
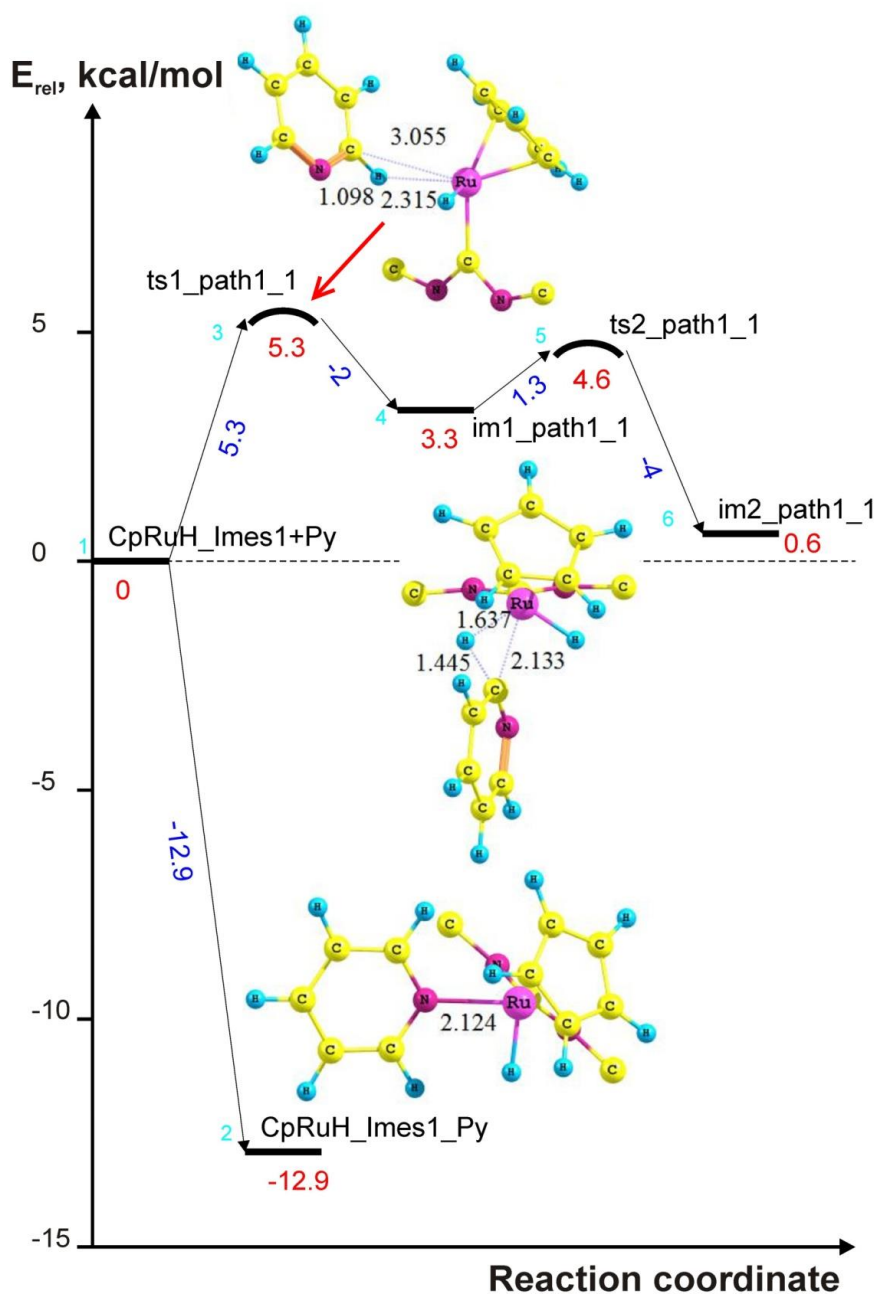
Figure S21. Relative energy profile for pyridine addition reaction catalyzed by Cp(L)RuH for the major and catalyst inhibition channels. The bond lengths are given in Å.

The inhibition of catalysis by added carbene was studied. We considered an associative pathway. Addition of the model carbene L to the intermediate **11** generates the bis(carbene) complex $Cp(L)_2RuH$ (**12**). Formation of **12** is an exothermic process ($\Delta_rE = -3.70$ kcal/mol, $\Delta_rG(50°C) = 18.00$ kcal/mol).

Figure S22. Bis(carbene) complex Cp(IMes)$_2$RuH (**15**).

5. References

[1] S. H. Lee, S. I. Gorelsky and G. I. Nikonov, *Organometallics*, 2013, **32**, 6599-6604.

[2] V. H. Mai, L. G. Kuzmina, A. V. Churakov, I. Korobkov, J. A. K. Howard and G. I. Nikonov, *Dalton Transactions*, 2016, **45**, 208-215.
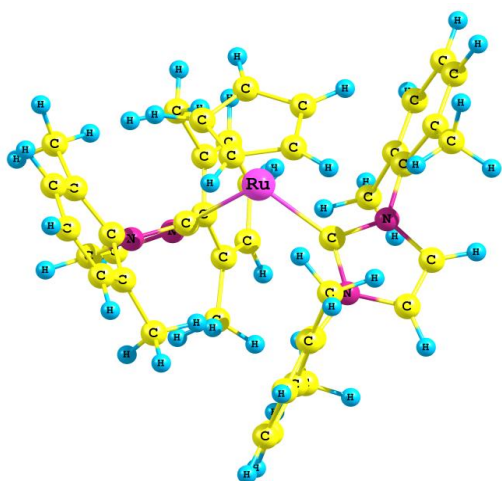
[3] A. L. Osipov, D. V. Gutsulyak, L. G. Kuzmina, J. A. K. Howard, D. A. Lemenovskii, G. Suess-Fink and G. I. Nikonov, *J. Organomet. Chem.*, 2007, **692**, 5081-5085.

[4] M. V. Basilevsky, A. G. Shamov, *Chem. Phys.*, 1981, **60**, 347-358.

[5] M. V. Basilevsky, *Chem. Phys.*, 1982, **67**, 337-346.

[6] M. V. Basilevsky, *J. Mol. Struct.*, 1983, **103**, 139-152.

[7] M. V. Basilevsky, *Pure. Appl. Chem.*, 1988, **55**, 207-212.

[8] O. B. Gadzhiev, S. K. Ignatov, A. G. Razuvaev and Artëm E. Masunov, *J. Phys. Chem. A*, 2009, **113**, 9092–9101.

[9] O. B. Gadzhiev, P. G. Sennikov, A. I. Petrov, D. Gogova and D. Siche, *Cryst. Growth Des.*, 2013, **13**, 1445–1457.

[10] O. B. Gadzhiev, P. G. Sennikov, A. I. Petrov, K. Kachel, S. Golka, D. Gogova and D. Siche, *J Mol Model.*, 2014, **20**, 2473-2485.

[11] Frisch, M. J.; Trucks, G. W.; Schlegel, H. B.; Scuseria, G. E.; Robb, M. A.; Cheeseman, J. R.; Montgomery, J. A., Jr.; Vreven, T.; Kudin, K. N.; Burant, J. C.; Millam, J. M.; Iyengar, S. S.; Tomasi, J.; Barone, V.; Mennucci, B.; Cossi, M.; Scalmani, G.; Rega, N.; Petersson, G. A.; Nakatsuji, H.; Hada, M.; Ehara, M.; Toyota, K.; Fukuda, R.; Hasegawa, J.; Ishida, M.; Nakajima, T.; Honda, Y.; Kitao, O.; Nakai, H.; Klene, M.; Li, X.; Knox, J. E.; Hratchian, H. P.; Cross, J. B.; Bakken, V.; Adamo, C.; Jaramillo, J.; Gomperts, R.; Stratmann, R. E.; Yazyev, O.; Austin, A. J.; Cammi, R.; Pomelli, C.; Ochterski, J. W.; Ayala, P. Y.; Morokuma, K.; Voth, G. A.; Salvador, P.; Dannenberg, J. J.; Zakrzewski, V. G.; Dapprich, S.; Daniels, A. D.; Strain, M. C.; Farkas, O.; Malick, D. K.; Rabuck, A. D.; Raghavachari, K.; Foresman, J. B.; Ortiz, J. V.; Cui, Q.; Baboul, A. G.; Clifford, S.; Cioslowski, J.; Stefanov, B. B.; Liu, G.; Liashenko, A.; Piskorz, P.; Komaromi, I.; Martin, R. L.; Fox, D. J.; Keith, T.; Al-Laham, M. A.; Peng, C. Y.; Nanayakkara, A.; Challacombe, M.; Gill, P. M. W.; Johnson, B.; Chen, W.; Wong, M. W.; Gonzalez, C.; Pople, J. A. Gaussian 03, Version D.02; Gaussian, Inc.: Wallingford, CT, 2007.